Effect of reduced graphene oxide hybridization on ZnO nanoparticles sensitivity to NO_2 gas: A DFT study

M. A. Abdulsattar[a,b,*], M. T. Hussein[c], M. U. Kahaly[d,e]
[a]*Department of Pharmacy, Al-Rasheed University College, Baghdad, Iraq*
[b]*Ministry of Science and Technology, Baghdad, Iraq*
[c]*Department of Physics, College of Science, University of Baghdad, Baghdad, Iraq*
[d]*ELI-ALPS, ELI-HU Non-Profit Ltd., Szeged, Hungary*
[e]*Institute of Physics, University of Szeged, Dóm tér 9, Szeged, 6720, Hungary*

In the present work, a density functional theory (DFT) calculation to simulate reduced graphene oxide (rGO) hybrid with zinc oxide (ZnO) nanoparticle's sensitivity to NO_2 gas is performed. In comparison with the experiment, DFT calculations give acceptable results to available bond lengths, lattice parameters, X-ray photoelectron spectroscopy (XPS), energy gaps, Gibbs free energy, enthalpy, entropy, etc. to ZnO, rGO, and ZnO/rGO hybrid. ZnO and rGO show n-type and p-type semiconductor behavior, respectively. The formed p-n heterojunction between rGO and ZnO is of the staggering gap type. Results show that rGO increases the sensitivity of ZnO to NO_2 gas as they form a hybrid. ZnO/rGO hybrid has a higher number of vacancies that can be used to attract oxygen atoms from NO_2 and change the resistivity of the hybrid. The combined reduction of oxygen from NO_2 and NO can give a very high value of the Gibbs free energy of reaction that explains the ppb level sensitivity of the ZnO/rGO hybrid. The dissociation of NO_2 in the air reduces the sensitivity of the ZnO/rGO hybrid at temperatures higher than 300℃.

(Received December 20, 2022; Accepted March 4, 2023)

Keywords: Reduced graphene oxide, ZnO; NO_2, Gas sensor, Density functional theory

1. Introduction

Reduced graphene oxide (rGO) is a material of high interest with simple methods to manufacture and numerous applications [1–3]. One of the contemporary applications of rGO is in gas sensors [4–6]. RGO offers several properties to enhance gas sensing that includes a wide area [7,8] and a high number of oxygen vacancies [9,10]. The wide area offered by rGO can increase the area even after mixing with another material which is also the case for the number of vacancies. The change in resistivity of rGO alone is very small when exposed to gases [11]. However, the resistivity of rGO hybrid with materials such as SnO_2, ZnO, NiO, or Pt changes rapidly with exposure to sensed gases that can reach parts-per-billion of gas concentration [11–13].

Zinc oxide (ZnO) is one of the most investigated materials with numerous applications [14,15]. Applications of ZnO include ceramics, coatings, medical, cigarette filters, food additives, etc. In addition to these applications, gas sensing is one of the important applications that proved to be applicable to many gases such as H_2S, H_2, NO_2, and CO_2 [16–19]. The ZnO/rGO hybrid proved to be beneficial in many research areas, including gas sensing [20,21].

NO_2 gas sensing is a contemporary research direction [22,23]. The reason for this interest in NO_2 gas is its health effects and wide pollution [24,25]. The NO_2 pollution effects are derived from many sources such as internal combustion engines and gas stoves that increase the exposure to NO_2 gas [26,27].

Density functional theory (DFT) has been a major rule in the development of a wide range of phenomena in several areas of science that begin in mathematics and do not end in medicine [28–30]. The use of DFT in gas sensing showed advances in understanding the gas sensing

* Corresponding author: mudarahmed3@yahoo.com
https://doi.org/10.15251/JOR.2023.192.153

phenomenon [31–33]. Recent development in DFT calculations, such as dispersion corrections, has also impacted gas sensing theories [34].

The literature of using rGO/ZnO in sensing NO_2 gas is limited to a few articles [12,35–38]. All the literature is after 2018. Some articles in the literature claim the possibility of reaching part per billion (ppb) detection limit at room temperature [37]. The reason for this precise detection limit will be obvious as we follow the results of present work. The available DFT calculations on rGO/ZnO detection of NO_2 does not rely on thermodynamic quantities described in the present work [37,39].

In the present work, NO_2 gas sensing using ZnO/rGO hybrid is discussed using DFT calculations. DFT calculations include ZnO, rGO, and ZnO/rGO hybrid. The results include bond lengths, X-ray photoelectron spectroscopy (XPS), energy gaps, etc. Reaction thermodynamic quantities such as Gibbs free energy, enthalpy, and entropy are also evaluated to back up the sensing mechanism of NO_2 gas in comparison with other gases such as H_2, CH_4, CO, and NO.

2. Theory

The electronic structure and physical properties of the three materials discussed in the present work, i.e., ZnO, rGO, and ZnO/rGO hybrid, are calculated. The sensitivity of these materials to NO_2 gas is discussed through the evaluation of their reaction thermodynamic energies, i.e., Gibbs free energy, enthalpy, and entropy. B3LYP method in DFT is frequently used in gas sensing simulations that include ZnO particles [40,41]. Several other DFT methods were used to evaluate ZnO electronic structure, ending by choosing B3LYP as one of the best of these methods [42]. The same method (B3LYP) is also used frequently used in DFT calculations that include rGO [43–45]. Choosing basis sets depends on the complexity and the number of atoms to be handled, especially the ZnO/rGO hybrid. The total number of atoms used to simulate the ZnO/rGO hybrid is 60 atoms. 6-311G** basis sets are our choice to perform the computational tasks. These basis sets give good results in comparison with the computer time needed to perform these calculations.

Small clusters of ZnO in the wurtzite structure are called wurtzoids [46–48]. These wurtzoids vary in shape and size. However, we must choose the right size so that we can perform our calculations without being stuck with inappropriate program execution times. The best-chosen size is called ZnO wurtzoid2c ($Zn_{13}O_{13}$), shown in Fig. (1a). ZnO wurtzoids have been successfully used in solving gas sensing calculations [47,49–51].

Coronene ($C_{24}H_{12}$) is used frequently to mimic rGO [52,53]. However, the edges of rGO do not have to be passivated with hydrogen only as in coronene. As a result, we chose to passivate the edges by a hydroxyl group (O.H.) in addition to H, as in Fig. (1b). Some edges are left without passivation, as expected empirically due to the removal of oxygen in the oxygen reduction process of rGO.

The interaction of ZnO with rGO is shown in Fig. (1c), as we can see from this figure that some oxygen atoms in ZnO are pulled by rGO because of oxygen deficiency in rGO. Some carbon atoms are also connected to zinc atoms to drag more electrons from the ZnO cluster. The effects on the final properties of the ZnO/rGO hybrid are discussed in detail in the next section.

Gaussian 09 program [54] is used to carry out the present work calculations, including dispersion corrections that should be important in NO_2 gas sensing phenomena [55,56]. This correction at the GD3BJ level is added [57].

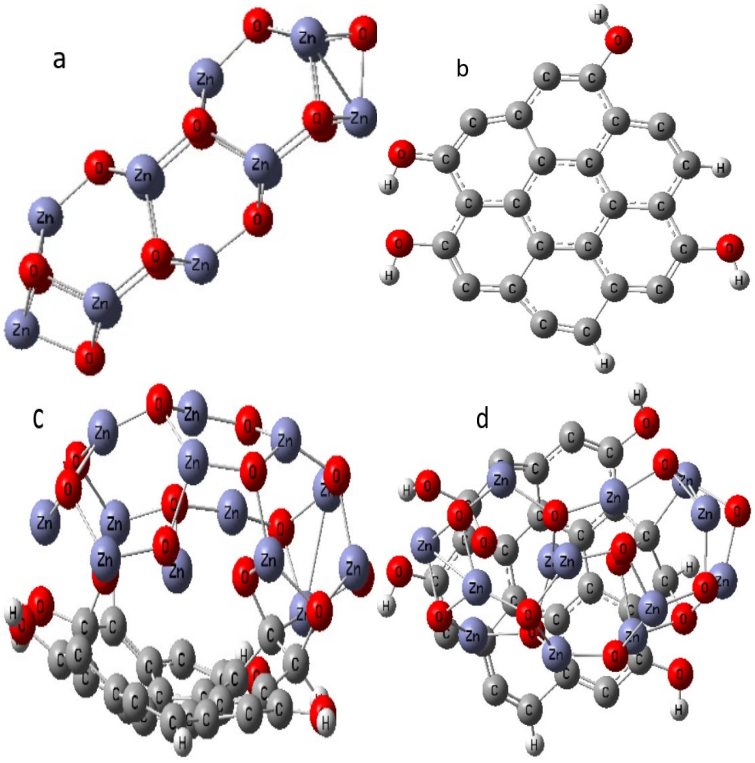

Fig. 1. (a) $Zn_{13}O_{13}$ cluster molecule, (b) reduced graphene oxide (rGO) cluster molecule, (c) ZnO/rGO hybrid side view, (d) ZnO/rGO hybrid upper view.

For a reaction in the form:

$$\alpha A + \beta B \rightarrow \rho R. \tag{1}$$

The equilibrium constant (K_{eq}) is given by [58]:

$$K_{eq} = \frac{[R]^{\rho}}{[A]^{\alpha}[B]^{\beta}} \tag{2}$$

In the above equation, [A] is the concentration of A reactant. In addition, the equilibrium constant is connected to the change in Gibbs free energy of reaction for one molecule (ΔG), Boltzmann constant (k), and temperature (T) by the relation [59]:

$$K_{eq} = e^{\frac{-\Delta G}{kT}} \tag{3}$$

The change in Gibbs free energy is connected to the change in enthalpy (ΔH) and entropy energy (TΔS) by the relation [60]:

$$\Delta G = \Delta H - T\Delta S \tag{4}$$

The above equations can be used to determine the number of active reaction sites for the reaction of a gas molecule in the sensing material, as we shall see in the results section. The reaction rate is also an important quantity that will be needed in the results section. The reaction rate of Eq. (1) can be given by [61]:

$$\frac{d[A]}{dt} = -k(T)[A]^{\alpha}[B]^{b}. \tag{5}$$

In the above equation, a and b are usually related to the α and β in Eq. (1). k(T) is the reaction rate constant that depends on the kind of theory used to solve the reaction problem. Generally, k(T) can be given by [62]:

$$k(T) = CT^{\alpha} \exp^{\left(\frac{-E_a}{k_B T}\right)}. \quad (6)$$

In the above equation, C is a constant, and α depends on the reaction theory. As an example, α is equal to 0 in Arrhenius's theory. E_a is the activation energy in Arrhenius's theory. It is also called Gibbs free energy of activation in transition state theory [63].

3. Results and discussion

Table 1 shows some of the properties of ZnO, and rGO and ZnO/rGO hybrid calculated in the present DFT calculations in comparison with available experimental findings. These include bond lengths, lattice constants, energy gaps, and X-ray photoelectron spectroscopy (XPS). In the present work, theoretical results have an acceptable agreement with experimental results since both two methods (DFT and experiment) contain probable errors.

Table 1. Calculated ZnO, rGO, and ZnO/rGO hybrid properties in comparison with available experimental values. Lattice constants and bond lengths are taken near the center of molecules.

Quantity	Theoretical (Present work)	Experimental	Experimental references
Zn-O bond length Å	1.850 to 1.918	1.82 to 2.01	[64–66]
ZnO lattice constant (a) Å	3.194	3.25	[67]
ZnO lattice constant (c) Å	5.377	5.2	[67]
ZnO energy gap eV	3.117	3.26	[68]
C-C bond length in rGO Å	1.424	1.42	[69]
rGO lattice constant (a) Å	2.466	2.46	[69]
rGO energy gap eV	1.248	1.00 to 1.69	[70]
ZnO/rGO energy gap eV	1.302	-	-
XPS rGO O1s eV	-521.586 to -521.961	-531.19 to -533.8	[71]
XPS ZnO O1s eV	-517.324 to -518.085	-532.6	[12]
XPS ZnO/rGO O1s eV	-517.528 to -521.948	-	-

ZnO wurtzoids are the stable molecules of ZnO at the molecular scale that reflect the wurtzite structure. However, these molecules are in an atmosphere that contains oxygen molecules that can react with ZnO. Our model molecule $Zn_{13}O_{13}$ can have one of the two following reactions (all reactions are at standard conditions of 25 ℃ and 1 atm unless otherwise mentioned):

$$Zn_{13}O_{13} + ½O_2 \rightarrow Zn_{13}O_{14}, (\Delta G = 2.209 \text{ eV}). \quad (7)$$

$$Zn_{13}O_{13} \rightarrow ½O_2 + Zn_{13}O_{12}, (\Delta G = 1.153 \text{ eV}). \quad (8)$$

As we can see from the above two reactions, energetically, ZnO prefers to stay at the stoichiometry $Zn_{13}O_{13}$ since losing or accepting oxygen atoms is an unfavorable reaction with positive Gibbs free energy. However, statistically, it is easier energetically (lower Gibbs free energy (ΔG= 1.153 eV)) to lose oxygen and forms oxygen vacancies which is the reason that intrinsic ZnO is an n-type semiconductor [72]. On the other hand, rGO can only accept oxygen because of the removal of oxygen in the reduction process. As a result, rGO is a p-type semiconductor [73]. Fig. 2 shows the energy gap of the ZnO cluster/rGO cluster before and after forming the ZnO/rGO hybrid. The formed heterojunction is of a staggering gap.

In the present theory, the interaction of the ZnO cluster with NO_2 gas can be given by the equation:

$$Zn_{13}O_{13}+NO_2 \rightarrow Zn_{13}O_{14}+NO, (\Delta G= 2.625 \text{ eV}). \quad (9)$$

As we can see from the above reaction, the Gibbs free energy of the reaction is high and of a positive value so that the reaction is an endergonic reaction or unfavorable reaction. On the other hand, the reaction of ZnO cluster with hydrogen molecule is an exergonic reaction as in the following:

$$Zn_{13}O_{13}+H_2 \rightarrow Zn_{13}O_{12}+H_2O, (\Delta G= -0.819 \text{ eV}). \quad (10)$$

H_2 is not the only gas that has an exergonic reaction; other gases such as CH_4, CO, CH_2O, NH_3, etc., also behave in the same manner. Fig. 3 shows some of these gases in comparison with NO_2, as we can see from Fig. 3, the ZnO cluster is not sensitive to NO_2 gas due to the high energy needed to be supplied for its endergonic reaction. Other gases such as H_2, CO, or CH_4 can be sensitized due to their exergonic reactions. On the other hand, the reaction of these gases with the ZnO/rGO cluster hybrid is totally different, as in Fig. 4.

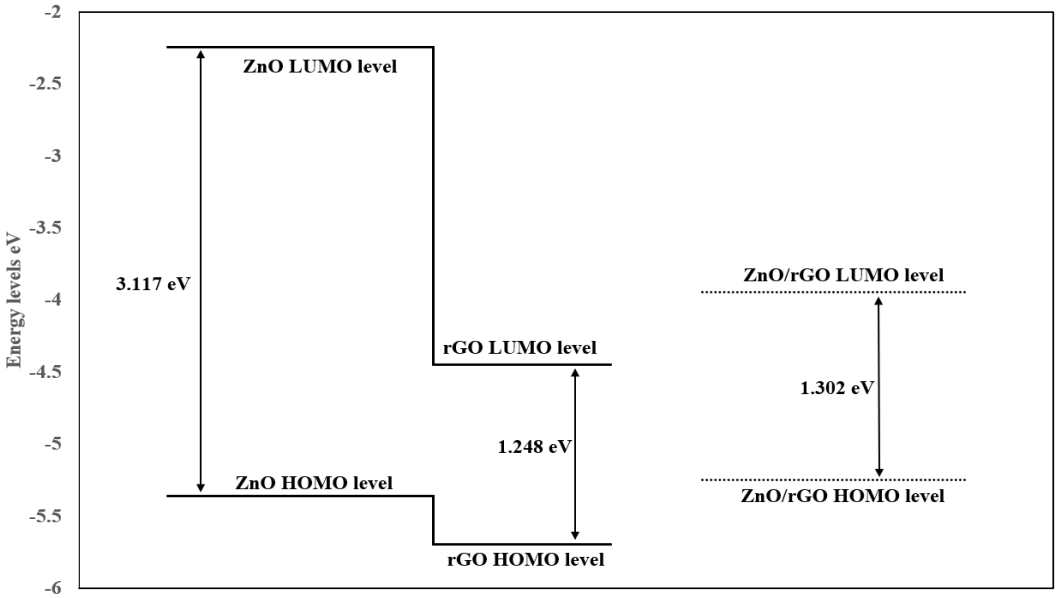

Fig. 2. Energy gap, HOMO, and LUMO levels of ZnO and rGO clusters before and after the formation of ZnO/rGO hybrid.

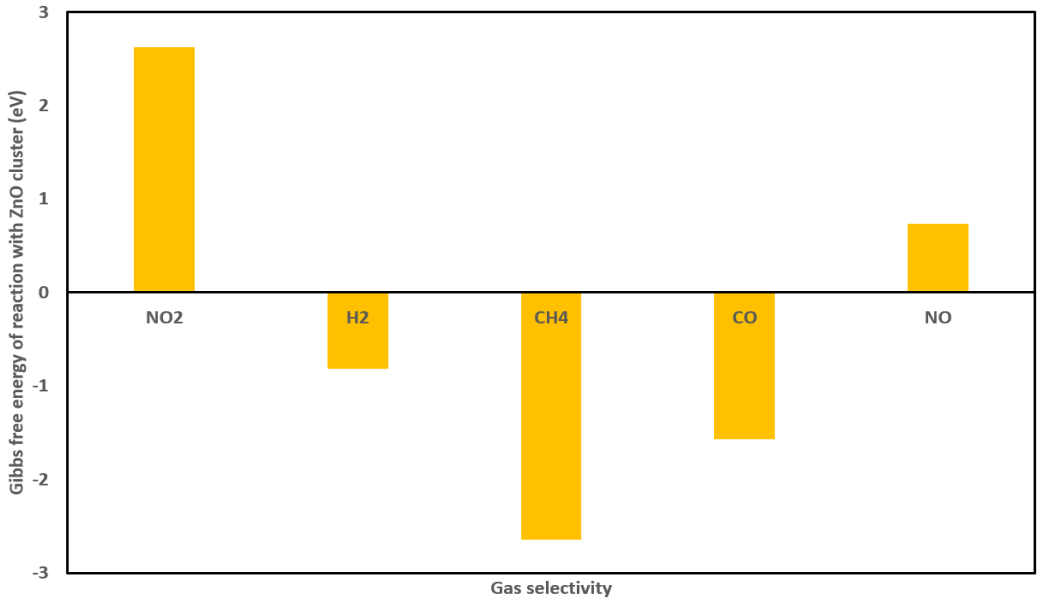

Fig. 3. Gibbs free energy of reaction of ZnO cluster ($Zn_{13}O_{13}$) with different gas molecules. Energies are per one molecule of the gas.

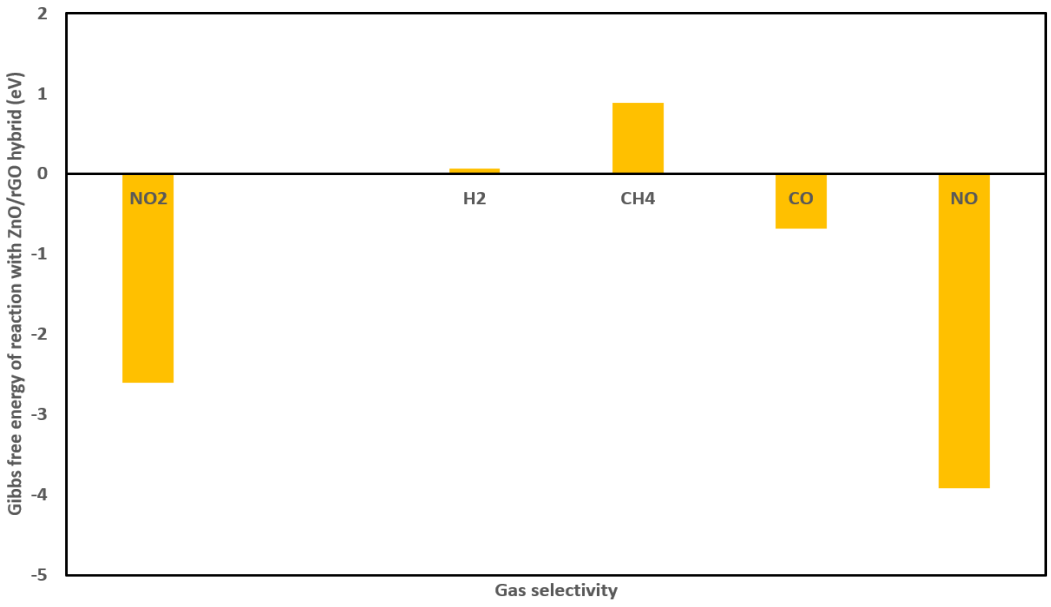

Fig. 4. Gibbs free energy of reaction of ZnO/rGO cluster hybrid ($Zn_{13}O_{13}/C_{24}O_4H_6$) with different gas molecules. Energies are per one molecule of the gas.

Most oxygen is removed from the rGO cluster so that it is in high need of oxygen. This is also reflected in the ZnO/rGO cluster hybrid. The high number of oxygen vacancies in the ZnO/rGO cluster makes the reaction with NO_2 oxidizing gas more favorable, while the reaction of oxygen reducing gases becomes unfavorable, as can be seen in Fig. 4.

The properties of the sensed gas are of great importance in the sensing operation [74]. NO_2 gas decomposes at temperatures well below room temperature as it passes over a catalyst such as Ag [75]. This decomposition explains that most NO_2 sensors operate at temperatures lower than 300℃ [13]. In fact, many NO_2 sensors operate at room temperature (R.T.) [76]. The decomposition of NO_2 as it approaches the sensor surface (sensor surface acts as a catalyst in this

case) decreases the sensitivity rapidly as we go higher in temperature, making optimum temperatures to be between R.T. and 300℃.

Table 2 shows the thermodynamic energies that include Gibbs free energy, enthalpy, and entropy for the various reactions encountered in the present calculations. The entropy can be given by the equation [77]:

$$S=k_B \ln(\Omega). \quad (11)$$

In the above equation, Ω is the number of microstates of a given energy level. This equation can explain the trends in Table 2.

Table 2. Gibbs free energies, enthalpies, and entropies energies of reactions at standard temperature (298.15 Kelvin) and pressure (1 atm). Energies are per one molecule of the interacting gas.

n	Reaction	ΔG (eV)	ΔH (eV)	TΔS (eV)
1	$Zn_{13}O_{13}+NO_2 \rightarrow Zn_{13}O_{14}+NO$	2.625	2.655	0.030
2	$Zn_{13}O_{13}+H_2 \rightarrow Zn_{13}O_{12}+H_2O$	-0.819	-0.643	0.175
3	$4Zn_{13}O_{13}+CH_4 \rightarrow 4Zn_{13}O_{12}+CO_2+2H_2O$	-2.646	-1.478	1.168
4	$Zn_{13}O_{13}+CO \rightarrow Zn_{13}O_{12}+CO_2$	-1.568	-1.523	0.045
5	$Zn_{13}O_{13}+NO \rightarrow Zn_{13}O_{12}+NO_2$	0.737	0.839	0.102
6	$Zn_{13}O_{13}/C_{24}O_4H_6+NO_2 \rightarrow Zn_{13}O_{14}/C_{24}O_4H_6+NO$	-2.607	-2.663	-0.056
7	$Zn_{13}O_{13}/C_{24}O_4H_6+H_2 \rightarrow Zn_{13}O_{12}/C_{24}O_4H_6+H_2O$	0.063	0.175	0.112
8	$4Zn_{13}O_{13}/C_{24}O_4H_6+CH_4 \rightarrow 4Zn_{13}O_{12}/C_{24}O_4H_6+CO_2+2H_2O$	0.879	1.794	0.915
9	$Zn_{13}O_{13}/C_{24}O_4H_6+CO \rightarrow Zn_{13}O_{12}/C_{24}O_4H_6+CO_2$	-0.686	-0.704	-0.0180
10	$Zn_{13}O_{13}/C_{24}O_4H_6+NO \rightarrow Zn_{13}O_{14}/C_{24}O_4H_6+½N_2$	-3.915	-4.202	-0.287
11	$NO_2 \rightarrow NO+½O_2$	0.416	0.626	0.209
12	$NO_2 \rightarrow ½N_2+O_2$	-0.475	-0.287	0.188

The first five reactions in Table 2 correspond to the reaction of different gases with the pure ZnO cluster that is visualized in Fig. 3. All reactions are normalized to one molecule of the reacting gas. All enthalpies of the first five reactions are close in their values to the free energy values except the third reaction. In the third reaction, the number of product molecules is higher than the interacting molecules, which increases the number of microstates and hence the entropy of reaction as in Eq. (11). The increase in the entropy of the reaction increases the difference between free energy and enthalpy, as in Eq. (4). The third reaction (CH_4 reaction) is also the most favorable reaction with the ZnO cluster since it consumes the oxygen from four ZnO clusters, as is obvious from the third reaction equation in Table 2. The first five reactions in Table 2 show that neither NO_2 nor its reaction product NO is favorable reactions with pure ZnO cluster. On the other hand, reactions 6 to 10 in Table 2 for the reaction of different considered gases with ZnO/rGO cluster hybrid show entirely different behavior, as visualized in Fig. 4. The most favorable reaction is with the NO and NO_2 gases, followed by C.O. gas. As a result, NO gas will interfere with ZnO/rGO cluster hybrid sensitivity to NO_2 gas. The combined effect of oxygen reduction from NO_2 and NO has a Gibbs free energy of -6.521 eV, which explains why the sensitivity to NO_2 gas can reach ppb level [12]. The other gas (in the investigated gases) that will interfere with NO_2 gas is C.O. However, as we recognize from Eq. (6), the Gibbs free energy of the reaction is in the exponent part of this equation. As a result, the interference between NO_2 and C.O. gases will be limited due to the large difference between their Gibbs free energies of reaction with the ZnO/rGO cluster hybrid.

The last two reactions in Table 2 are the dissociation of NO_2 to NO or N_2 and oxygen. The dissociation rate in R.T. is low, as can be seen from the values of Gibbs free energies of reaction. However, it increases with temperature, as in Eq. (6). This increase will lower the concentration of NO_2 near the sensor surface and finally decreases the reaction rate and sensitivity of the sensor to NO_2 gas as in Eq. (5) at temperatures higher than 300℃ [13]. Due to the existence of NO and NO_2 always together that accompany NO_2 dissociation, the term NO_x is frequently used [78].

4. Conclusions

Calculations using DFT proves that ZnO/rGO cluster hybrid has high sensitivity and selectivity to NO_2 gas than the pure ZnO cluster. The calculations are used first to prove that the simulation of ZnO and rGO clusters gives good theoretical results of several experimental properties such as bond lengths, lattice parameters, XPS, energy gaps, Gibbs free energy, enthalpy, and entropy. A p-n heterojunction between rGO and ZnO of the staggering gap type is formed after mixing. The mixing of ZnO and rGO increases the number of oxygen vacancies in the ZnO cluster due to the pulling of oxygen atoms from ZnO to rGO. Oxygen deficiency in ZnO/rGO increases its reaction and sensitivity to oxidizing gases such as NO_2 and reduces its reaction and sensitivity to oxygen-reducing gases such as H_2, CH_4, and C.O. The combined reduction of oxygen from NO_2 and NO can give a very high value of the free energy that explains the ppb level sensitivity of the ZnO/rGO hybrid. NO_2 gas dissociation reduces NO_2 sensitivity in temperatures greater than 300℃.

References

[1] C. Krishnaraj, V.K. Kaliannagounder, R. Rajan, T. Ramesh, C.S. Kim, C.H. Park, B. Liu, S.-I. Yun, Environ. Res. 210 (2022); https://doi.org/10.1016/j.envres.2022.112864

[2] S. Sengupta, A. Pari, L. Biswas, P. Shit, K. Bhattacharyya, A.P. Chattopadhyay, Biointerface Res. Appl. Chem. 12 (2022) 6196-6210; https://doi.org/10.33263/BRIAC125.61966210

[3] W. Zhang, H. Xu, F. Xie, X. Ma, B. Niu, M. Chen, H. Zhang, Y. Zhang, D. Long, Nat. Commun. 13 (2022); https://doi.org/10.1038/s41467-022-28180-4

[4] A. Umar, A.A. Ibrahim, H. Algadi, H. Albargi, M.A. Alsairi, Y. Wang, S. Akbar, Environ. Technol. Innov. 25 (2022); https://doi.org/10.1016/j.eti.2021.102066

[5] H. Park, W. Kim, S.W. Lee, J. Park, G. Lee, D.S. Yoon, W. Lee, J. Park, J. Mater. Sci. Technol. 101 (2022) 165-172; https://doi.org/10.1016/j.jmst.2021.06.018

[6] S. He, Y. Liu, W. Feng, B. Li, X. Yang, X. Huang, Meas. Sci. Technol. 33 (2022); https://doi.org/10.1088/1361-6501/ac39d3

[7] S.H. Hwang, Y.-B. Park, H.J. Ahn, J.-C. Yoon, J.-H. Jang, Int. SAMPE Tech. Conf., 2013: pp. 1780-1790.

[8] J. Vanek, R. Mach, ECS Trans., 2018: pp. 253-259; https://doi.org/10.1149/08701.0253ecst

[9] M. Zhang, H. Sun, Y. Guo, D. Wang, D. Sun, Q. Su, S. Ding, G. Du, B. Xu, J. Mater. Sci. 56 (2021) 7573-7586; https://doi.org/10.1007/s10853-020-05747-4

[10] J. Hou, T. Zhang, T. Jiang, X. Wu, Y. Zhang, M. Tahir, A. Hussain, M. Luo, J. Zou, X. Wang, J. Clean. Prod. 328 (2021); https://doi.org/10.1016/j.jclepro.2021.129651

[11] J.-Y. Kang, W.-T. Koo, J.-S. Jang, D.-H. Kim, Y.J. Jeong, R. Kim, J. Ahn, S.-J. Choi, I.-D. Kim, Sensors Actuators, B Chem. 331 (2021); https://doi.org/10.1016/j.snb.2020.129371

[12] P. Cao, Y. Cai, D. Pawar, S.T. Navale, C.N. Rao, S. Han, W. Xu, M. Fang, X. Liu, Y. Zeng, D. Zhu, Y. Lu, Chem. Eng. J. 401 (2020); https://doi.org/10.1016/j.cej.2020.125491

[13] S. Bai, J. Han, J.C. Meng, L. Sun, J. Sun, Y. Zhao, P. Tang, R. Luo, D. Li, A. Chen, Sensors Actuators, B Chem. 339 (2021); https://doi.org/10.1016/j.snb.2021.129720

[14] M.R.A. Bhuiyan, H. Mamur, Iran. J. Mater. Sci. Eng. 18 (2021).

[15] D. Kumar, Eng. Res. Express. 3 (2021); https://doi.org/10.1088/2631-8695/ac3b29

[16] Y. Nagarjuna, Y.-J. Hsiao, J. Electrochem. Soc. 168 (2021); https://doi.org/10.1149/1945-7111/ac0aa8

[17] S. Agarwal, S. Kumar, H. Agrawal, M.G. Moinuddin, M. Kumar, S.K. Sharma, K. Awasthi, Sensors Actuators B Chem. 346 (2021); https://doi.org/10.1016/j.snb.2021.130510

[18] X. Ren, Z. Xu, D. Liu, Y. Li, Z. Zhang, Z. Tang, Sensors Actuators B Chem. 357 (2022); https://doi.org/10.1016/j.snb.2022.131384

[19] T. Bhowmick, A. Ghosh, S. Nag, S.B. Majumder, J. Alloys Compd. 903 (2022); https://doi.org/10.1016/j.jallcom.2022.163871

[20] A. Landström, A. Gradone, R. Mazzaro, V. Morandi, I. Concina, Ceram. Int. 47 (2021) 19346-19355; https://doi.org/10.1016/j.ceramint.2021.03.271
[21] P.C. Nethravathi, D. Suresh, Inorg. Chem. Commun. 134 (2021); https://doi.org/10.1016/j.inoche.2021.109051
[22] T. Li, D. Zhang, Q. Pan, M. Tang, S. Yu, Sensors Actuators B Chem. 355 (2022); https://doi.org/10.1016/j.snb.2021.131049
[23] W. Li, Q. Ou, X. Wang, K. Xing, T. Tesfamichael, N. Motta, D.-C. Qi, Appl. Surf. Sci. 586 (2022); https://doi.org/10.1016/j.apsusc.2022.152793
[24] M.G. Ghozikali, A. Borgini, A. Tittarelli, A. Amrane, K. Naddafi, M. Mohammadyan, G. Goudarzi, R. Bono, B. Heibati, Fresenius Environ. Bull. 24 (2015) 4142-4148.
[25] M.S. Hossain, H.C. Frey, P.K.K. Louie, A.K.H. Lau, Environ. Pollut. 270 (2021); https://doi.org/10.1016/j.envpol.2020.116280
[26] R. Bichler, M. Bittner, Atmos. Environ. 272 (2022); https://doi.org/10.1016/j.atmosenv.2022.118948
[27] Y. Zhang, R. Zhou, J. Chen, N. Rangel-Buitrago, Ocean Coast. Manag. 219 (2022); https://doi.org/10.1016/j.ocecoaman.2022.106064
[28] P. Morgante, R. Peverati, Int. J. Quantum Chem. 120 (2020); https://doi.org/10.1002/qua.26332
[29] Z. Tao, X. Xu, L. Bi, Electrochem. Commun. 129 (2021); https://doi.org/10.1016/j.elecom.2021.107072
[30] S. Mahmoudi, M.M. Dehkordi, M.H. Asgarshamsi, J. Mol. Model. 27 (2021); https://doi.org/10.1007/s00894-021-04891-1
[31] D. Chakraborty, V. Kumar, S.M. Kamil, P. Johari, Using ACS Appl. Nano Mater. (2021); https://doi.org/10.1021/acsanm.1c00846
[32] Q. Pan, T. Li, D. Zhang, Sensors Actuators, B Chem. 332 (2021); https://doi.org/10.1016/j.snb.2021.129440
[33] K.O. Obodo, C.N.M. Ouma, J.T. Obodo, G. Gebreyesus, D.P. Rai, A.M. Ukpong, B. Bouhafs, Nanotechnology. 32 (2021); https://doi.org/10.1088/1361-6528/ac04d0
[34] V. Babar, S. Sharma, U. Schwingenschlögl, J. Phys. Chem. C. 124 (2020) 5853-5860; https://doi.org/10.1021/acs.jpcc.9b10553
[35] Jyoti, N. Kanaujiya, G.D. Varma, AIP Conf. Proc., 2018; https://doi.org/10.1063/1.5032374
[36] H. Gao, Y. Ma, P. Song, J. Leng, Q. Wang, J. Mater. Sci. Mater. Electron. 32 (2021) 10058-10069; https://doi.org/10.1007/s10854-021-05664-5
[37] Z. Chen, H. Guo, F. Zhang, X. Li, J. Yu, X. Chen, Adv. Mater. Interfaces. 8 (2021); https://doi.org/10.1002/admi.202101511
[38] M. Yuan, C. Peng, J. Fu, X. Liu, Z. Wang, S. Xu, S. Cui, J. Alloys Compd. 908 (2022); https://doi.org/10.1016/j.jallcom.2022.164567
[39] K. Ghosh, N.S. Mahapatra, H. Rahaman, P. Bhattacharyya, IEEE Trans. Nanotechnol. 18 (2019) 119-125; https://doi.org/10.1109/TNANO.2018.2884171
[40] H. Juwono, A.F. Imron, N.I. Oktavianti, A.L. Ivansyah, Y. Kusumawati, Monatshefte Fur Chemie. 153 (2022) 49-59; https://doi.org/10.1007/s00706-021-02879-4
[41] N.-Y. Xu, P.D. Kheirollahi Nezhad, J. Phys. Chem. Solids. 161 (2022); https://doi.org/10.1016/j.jpcs.2021.110379
[42] F.S. Saoud, J.C. Plenet, M. Henini, J. Alloys Compd. 619 (2015) 812-819; https://doi.org/10.1016/j.jallcom.2014.08.069
[43] B.B. Prasad, R. Singh, A. Kumar, Carbon N. Y. 102 (2016) 86-96; https://doi.org/10.1016/j.carbon.2016.02.031
[44] J.H. Yao, Z.L. Yin, Y.W. LiIOP Conf. Ser. Earth Environ. Sci., 2017; https://doi.org/10.1088/1755-1315/81/1/012026
[45] E.V. Gómez, N.A. Ramírez Guarnizo, J.D. Perea, A.S. López, J.J. Prías-Barragán, ACS Omega. 7 (2022) 3872-3880; https://doi.org/10.1021/acsomega.1c00963

[46] M.A. Abdulsattar, Superlattices Microstruct. 85 (2015) 813-819; https://doi.org/10.1016/j.spmi.2015.07.015
[47] M.A. Abdulsattar, H.M. Almaroof, Surf. Rev. Lett. 24 (2017); https://doi.org/10.1142/S0218625X18500087
[48] F.A. Hasan, M.T. Hussein, Mater. Today Proc., 2021: pp. 2638-2644; https://doi.org/10.1016/j.matpr.2020.12.593
[49] M.A. Abdulsattar, J. Mol. Model. 23 (2017); https://doi.org/10.1007/s00894-017-3309-9
[50] M.A. Abdulsattar, H.M. Almaroof, N.M. Almaroof, Optik (Stuttg). 219 (2020); https://doi.org/10.1016/j.ijleo.2020.165278
[51] M.A. Abdulsattar, R.H. Jabbar, H.H. Abed, H.M. Abduljalil, Optik (Stuttg). 242 (2021); https://doi.org/10.1016/j.ijleo.2021.167158
[52] E. Makkos, D. Bodrogi, D. Szieberth, Phys. Chem. Chem. Phys. 23 (2021) 24738-24749; https://doi.org/10.1039/D1CP02320A
[53] J.A. Tyson, V. Mirabello, D.G. Calatayud, H. Ge, G. Kociok-Köhn, S.W. Botchway, G. Dan Pantoş, S.I. Pascu, Adv. Funct. Mater. 26 (2016) 5641-5657; https://doi.org/10.1002/adfm.201601123
[54] M.J. Frisch, et al., Gaussian 09, Revision A.02, (2009).
[55] V. Babar, S. Sharma, U. Schwingenschlögl, Adv. Theory Simulations. 1 (2018); https://doi.org/10.1002/adts.201700008
[56] D.R. Roy, M.A. Zaeem, S. Thomas, V. Kumar, ACS Appl. Nano Mater. 3 (2020) 10073-10081; https://doi.org/10.1021/acsanm.0c02072
[57] E.-L. Zins, J. Phys. Chem. A. 124 (2020) 1720-1734; https://doi.org/10.1021/acs.jpca.9b09992
[58] M. Khalili Rad, H. Towfighi, Solvent Extr. Ion Exch. 38 (2020) 472-483; https://doi.org/10.1080/07366299.2020.1739811
[59] T. Liu, J. Dispers. Sci. Technol. 29 (2008) 335-339; https://doi.org/10.1080/01932690701716036
[60] J.H. Lee, D.H. Suh, Nucl. Eng. Technol. 53 (2021) 3711-3716; https://doi.org/10.1016/j.net.2021.06.006
[61] L. Lu, R. Wang, J. Xue, F. Chen, J. Chen, Sci. China, Ser. D Earth Sci. 48 (2005) 1690-1697; https://doi.org/10.1360/02yd0115
[62] Joseph W. Ochterski, Thermochemistry in Gaussian, (2000).
[63] N.K. Nambiar, D. Brindha, P. Punniyakotti, B.R. Venkatraman, S. Angaiah, Eng. Sci. 17 (2022) 167-175; https://doi.org/10.30919/es8d540
[64] F.M. Hassan, A.U.S.A. Najim, Surf. Rev. Lett. 28 (2021); https://doi.org/10.1142/S0218625X21501183
[65] B.M. Omkaramurthy, G. Krishnamurthy, Inorg. Nano-Metal Chem. 49 (2019) 375-384; https://doi.org/10.1080/24701556.2019.1661460
[66] C. Supatutkul, S. Pramchu, A.P. Jaroenjittichai, Y. Laosiritaworn,. Phys. Conf. Ser., 2017; https://doi.org/10.1088/1742-6596/901/1/012172
[67] J. Charlesbabu, K. Gopalakrishnan, M. Elango, K. Vasudevan, Inorg. Nano-Metal Chem. 47 (2017) 1298-1303; https://doi.org/10.1080/24701556.2016.1242627
[68] A.F. Abdulrahman, A.A. Barzinjy, S.M. Hamad, M.A. Almessiere, ACS Omega. 6 (2021) 31605-31614; https://doi.org/10.1021/acsomega.1c04105
[69] W. Yu, L. Sisi, Y. Haiyan, L. Jie, RSC Adv. 10 (2020) 15328-15345; https://doi.org/10.1039/D0RA01068E
[70] Z. Wang, Y. Zhang, S. Liu, T. Zhang, Sensors Actuators, B Chem. 222 (2016) 893-903; https://doi.org/10.1016/j.snb.2015.09.027
[71] R. Al-Gaashani, A. Najjar, Y. Zakaria, S. Mansour, M.A. Atieh, Ceram. Int. 45 (2019) 14439-14448; https://doi.org/10.1016/j.ceramint.2019.04.165
[72] B. Munir, E.Y. Muslih, J. King Saud Univ. - Eng. Sci. 33 (2021) 525-530; https://doi.org/10.1016/j.jksues.2020.06.003

[73] E. Ruiz, T. Gueye, C. Masson, C. Varenne, A. Pauly, J. Brunet, A.L. Ndiaye, Chemosensors. 9 (2021); https://doi.org/10.3390/chemosensors9120346

[74] M.A. Abdulsattar, H.H. Abed, R.H. Jabbar, N.M. Almaroof, J. Mol. Graph. Model. 102 (2021); https://doi.org/10.1016/j.jmgm.2020.107791

[75] W.X. Huang, J.M. White, Surf. Sci. 529 (2003) 455-470; https://doi.org/10.1016/S0039-6028(03)00332-7

[76] L. Qi, L. Yu, Z. Liu, F. Guo, Y.Q. Gu, X. Fan, J. Alloys Compd. 749 (2018) 244-249; https://doi.org/10.1016/j.jallcom.2018.03.298

[77] G. Jona-Lasinio, Brazilian J. Probab. Stat. 29 (2015) 494-501; https://doi.org/10.1214/14-BJPS266

[78] S. Nundy, T.-Y. Eom, K.-Y. Song, J.-S. Park, H.-J. Lee, Ceram. Int. 46 (2020) 19354-19364; https://doi.org/10.1016/j.ceramint.2020.04.278